A self-reinforcing HIF2α–miR-23a-3p–PHD1 circuit rewires oxygen sensing to sustain pulmonary endothelial barrier integrity

Chan Chen[1,2#], Suobei Li[1,2#], Meiqin Li[1,2], Ke Li[1,2], Jia Wei[1,2], Chao Liu[1,2], Wei Ruan[1,2*]

[1]Department of Anesthesiology, Second Xiangya Hospital, Central South University, Changsha, 410011, China.
[2]Anesthesiology Research Institute, Central South University, Changsha, 410011, China.

[#]These authors contributed equally.
[*]Correspondence to:
Wei Ruan, MD, PhD. Email: ruanwei2001@csu.edu.cn

Contents

Supplementary Note 1: Supplementary Figures

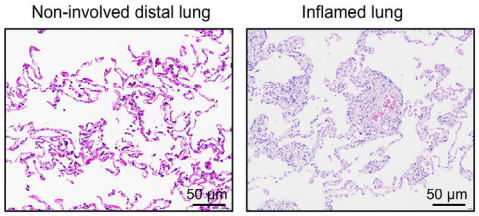

Supplementary Fig. 1. Histological review of human lung samples.
Representative H&E-stained sections show preserved alveolar parenchyma in non-involved distal lung controls and inflammatory infiltration/inflammatory injury in inflamed lung specimens, without tumor involvement in the analyzed regions. Scale bar, 50 µm. Images are representative of n = 6 non-involved distal lung specimens and n = 6 inflamed lung specimens.

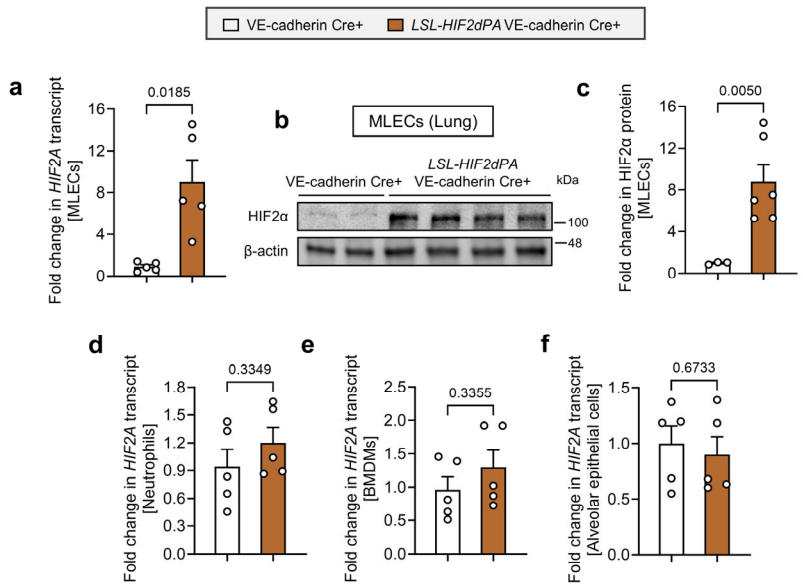

Supplementary Fig. 2. Confirmation of endothelial-specific overexpression of stabilized HIF2α in *LSL-HIF2dPA* VE-cadherin Cre+ mice.

a, *HIF2A* transcript levels in MLECs isolated from VE-cadherin Cre+ and *LSL-HIF2dPA* VE-cadherin Cre+ mice. n = 5 mice/group; unpaired two-tailed Welch's t-test. **b** and **c**, HIF2α protein levels in isolated MLECs. **b**, Western blot. **c**, Quantification. n = 3 VE-cadherin Cre+ mice and n = 6 *LSL-HIF2dPA* VE-cadherin Cre+ mice; unpaired two-tailed Welch's t-test. **d–f**, *HIF2A* transcript levels in neutrophils **(d)**, BMDMs **(e)**, and alveolar epithelial cells **(f)** isolated from VE-cadherin Cre+ and *LSL-HIF2dPA* VE-cadherin Cre+ mice. n = 5 mice/group; unpaired two-tailed t-tests. All samples are biologically independent. All data are mean ± s.e.m.

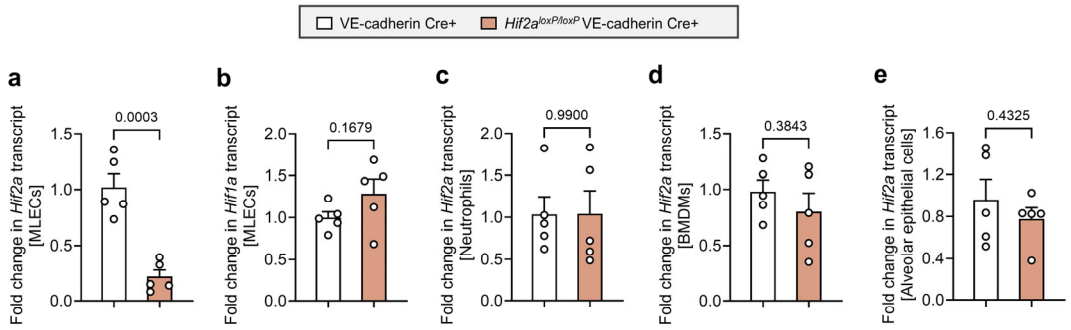

Supplementary Fig. 3. Confirmation of endothelial-specific deletion of *Hif2a* in *Hif2a*$^{loxP/loxP}$ VE-cadherin Cre+ mice.

a and **b**, *Hif2a* **(a)** and *Hif1a* **(b)** transcript levels in MLECs isolated from VE-cadherin Cre+ and *Hif2a*$^{loxP/loxP}$ VE-cadherin Cre+ mice. **c**–**e**, *Hif2a* transcript levels in neutrophils **(c)**, BMDMs **(d)**, and alveolar epithelial cells **(e)** isolated from VE-cadherin Cre+ and *Hif2a*$^{loxP/loxP}$ VE-cadherin Cre+ mice. n = 5 mice/group; unpaired two-tailed t-tests. All samples are biologically independent. All data are mean ± s.e.m.

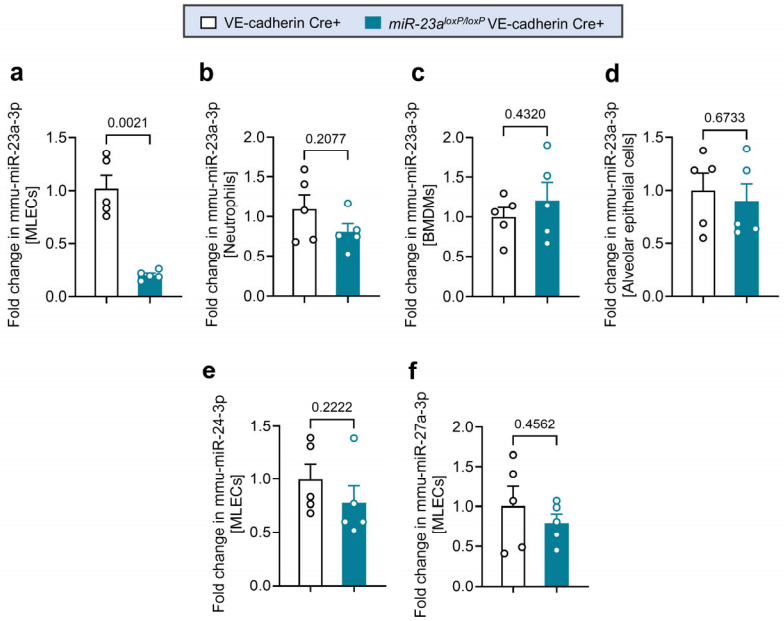

Supplementary Fig. 4. Confirmation of endothelial-specific deletion of miR-23a in *miR-23a*$^{loxP/loxP}$ VE-cadherin Cre+ mice.

a–d, Real-time PCR analysis of mature mmu-miR-23a-3p levels in isolated MLECs **(a)**, neutrophils **(b)**, BMDMs **(c)**, and alveolar epithelial cells **(d)** from VE-cadherin Cre+ and *miR-23a*$^{loxP/loxP}$ VE-cadherin Cre+ mice. **e** and **f**, mmu-miR-24-3p **(e)** and mmu-miR-27a-3p **(f)** levels in isolated MLECs from VE-cadherin Cre+ and *miR-23a*$^{loxP/loxP}$ VE-cadherin Cre+ mice. n = 5 mice/group; Welch's t-test was used for **a**, Mann-Whitney U test for **e**, and unpaired two-tailed t-tests were used for **b–d** and **f**. All samples are biologically independent. All data are mean ± s.e.m.

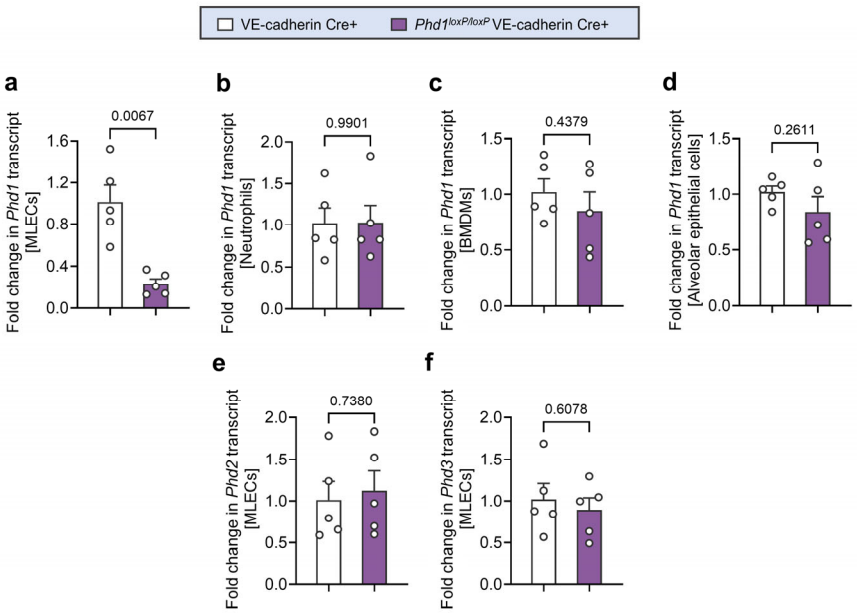

Supplementary Fig. 5. Confirmation of endothelial-specific deletion of *Phd1* in *Phd1*$^{loxP/loxP}$ VE-cadherin Cre+ mice.

a–d, Real-time PCR analysis of *Phd1* transcript levels in isolated MLECs **(a)**, neutrophils **(b)**, BMDMs **(c)**, and alveolar epithelial cells **(d)** from VE-cadherin Cre+ and *Phd1*$^{loxP/loxP}$ VE-cadherin Cre+ mice. **e** and **f**, *Phd2* **(e)** and *Phd3* **(f)** transcript levels in isolated MLECs from VE-cadherin Cre+ and *Phd1*$^{loxP/loxP}$ VE-cadherin Cre+ mice. n = 5 mice/group; Welch's t-test was used for **a**, and unpaired two-tailed t-tests were used for **b–f**. All samples are biologically independent. All data are mean ± s.e.m.

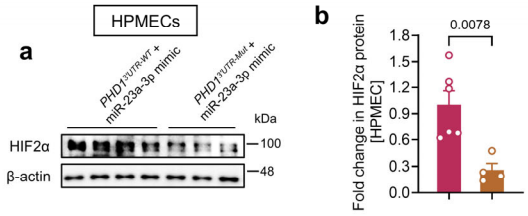

Supplementary Fig. 6. Disruption of the miR-23a-3p-responsive site in the *PHD1* 3′ UTR attenuates HIF2α accumulation.

HIF2α protein levels in HPMECs expressing $PHD1^{3'UTR\text{-}WT}$ or $PHD1^{3'UTR\text{-}Mut}$ after miR-23a-3p mimic treatment. **a**, Western blot. **b**, Quantification. n = 6 $PHD1^{3'UTR\text{-}WT}$ and n = 4 $PHD1^{3'UTR\text{-}Mut}$ biologically independent experiments; unpaired two-tailed t-test. All data are mean ± s.e.m.

Supplementary Note 2: Supplementary Tables

Supplementary Table 1. Clinicopathologic characteristics and experimental use of human lung specimens

Variable	Non-involved distal lung	Inflamed lung
Patient-level characteristics		
Number of subjects, n	6	6
Number of analyzed specimens/cases, n	6	6
Paired non-involved/inflamed specimens, n	0	0
Age, years, median (IQR)	57.5 (52–63)	54.5 (48–58)
Sex, male/female	4/2	3/3
Smoking status, never/former/current/unknown	2/3/1/0	2/2/2/0
Clinical diagnosis, n (%)	Localized primary lung tumor, 6 (100%)	Pulmonary inflammatory or infectious lesion, 6 (100%): pneumonia/inflammatory mass, 2 (33.3%); lung abscess, 1 (16.7%); bronchiectasis with active inflammation, 2 (33.3%); acute exacerbation of interstitial lung disease, 1 (16.7%)
Pathological diagnosis, n (%)	Histologically non-involved distal lung parenchyma from localized primary lung tumor resection specimens, 6 (100%); source tumor histology: adenocarcinoma, 4 (66.7%); squamous cell carcinoma, 2 (33.3%)	Active or recent inflammatory lung injury, 6 (100%): organizing pneumonia/active inflammatory injury, 2 (33.3%); suppurative inflammatory injury, 1 (16.7%); bronchiectasis with active inflammation, 2 (33.3%); interstitial pneumonia with acute inflammatory exacerbation, 1 (16.7%)
Specimen-level characteristics		
Anatomic site of resection	Upper lobe, 3; lower lobe, 3	Upper lobe, 2; right middle lobe/lingular segment, 1;

Variable	Non-involved distal lung	Inflamed lung
		lower lobe, 3
Indication for tissue acquisition	Clinically indicated surgical resection for localized primary lung tumor; distal non-involved parenchyma was sampled as comparator tissue	Clinically indicated thoracic surgery or surgical resection for pulmonary inflammatory or infectious lesions
Histological criteria for classification	Grossly and microscopically non-involved distal alveolar parenchyma, remote from tumor margin, without tumor infiltration or overt acute/chronic inflammation	Lung tissue with histological evidence of active or recent inflammatory injury, including inflammatory cell infiltration and inflammatory parenchymal injury
Specimen type, fresh-frozen/FFPE/both	0/0/6	0/0/6
Experimental use		
Use in bulk RNA/protein analysis, n	6	6
Use in miRNAscope/IF analysis, n	6	6

Data are presented as n, n (%) or median (IQR), as appropriate. FFPE, formalin-fixed paraffin-embedded; IF, immunofluorescence. Non-involved distal lung refers to histologically uninvolved lung parenchyma distant from the primary lesion. Inflamed lung refers to lung tissue with histological evidence of active or recent inflammatory injury. Number of analyzed specimens/cases refers to biologically independent subjects rather than separate tissue blocks or aliquots. Paired non-involved/inflamed specimens refers to matched comparator and inflamed lung tissues obtained from the same subject.

Supplementary Table 2. Consensus mmu-miR-23a-3p candidate target genes identified across four target resources. Provided as a separate Excel file.

Supplementary Table 3. Complete mmu-miR-23a-3p target-prediction matrix across miRanda, miRDB, TargetScan and CLIP-supported datasets. Provided as a separate Excel file.

Supplementary Table 4. miR-23a-3p candidate target network and confidence annotation. Provided as a separate Excel file.

Supplementary Table 5. Key resources table

REAGENT or RESOURCE	SOURCE	IDENTIFIER
Antibodies		
Anti-HIF1α antibody, rabbit monoclonal, clone BL-124-3F7	Bethyl Laboratories	Cat # A700-001
Anti-HIF1α antibody, mouse monoclonal, clone H1alpha67	Novus Biologicals	Cat # NB100-105
Anti-HIF2α antibody, rabbit monoclonal, clone BL-95-1A2	Bethyl Laboratories	Cat # A700-003
Anti-HIF2α antibody, rabbit polyclonal	Novus Biologicals	Cat # NB100-122
Anti-PHD1 antibody, rabbit polyclonal	Proteintech	Cat # 12984-1-AP
Anti-CD31 antibody, goat polyclonal	R&D Systems	Cat # AF3628
Anti-α-tubulin antibody, rabbit polyclonal	Cell Signaling Technology	Cat # 2144
Anti-β-actin antibody, mouse monoclonal, clone C4	Santa Cruz	Cat # sc-47778
Anti-GAPDH antibody, rabbit monoclonal, clone D16H11	Cell Signaling Technology	Cat # 5174
Lamin A/C, Mouse Monoclonal, clone 4C11	Cell Signaling Technology	Cat # 4777
Anti-mouse Ly6G antibody, clone 1A8	Bio X Cell	Cat # BE0075-1
Rat IgG2a isotype control antibody, clone 2A3	Bio X Cell	Cat # BE0089
TruStain FcX anti-mouse CD16/32 antibody, clone 93	BioLegend	Cat # 101320
B220-Alexa Fluor 488 antibody, clone RA3-6B2	BioLegend	Cat # 103228
CD3-FITC antibody, clone 17A2	BioLegend	Cat # 100203
Ly6G-APC/Cyanine7 antibody, clone 1A8	BioLegend	Cat # 127623
CD11b-Pacific Blue antibody, clone M1/70	BioLegend	Cat # 101223
CD11c-PE antibody, clone N418	BioLegend	Cat # 117307
Biotin anti-mouse CD16/CD32 antibody, clone 2.4G2	BD Biosciences	Cat # 553143
Biotin anti-mouse TER-119 antibody, clone TER-119	BD Biosciences	Cat # 553672

Biotin anti-mouse CD45 antibody, clone 30-F11	BD Biosciences	Cat # 553078
Biotin anti-mouse CD90.2 antibody, clone 30-H12	BD Biosciences	Cat # 553011
Alexa Fluor 594 donkey anti-goat IgG secondary antibody	Invitrogen/Thermo Fisher Scientific	Cat # A-11058
Alexa Fluor 488 donkey anti-rabbit IgG secondary antibody	Invitrogen/Thermo Fisher Scientific	Cat # A-21206
Alexa Fluor 488 donkey anti-mouse IgG secondary antibody	Invitrogen/Thermo Fisher Scientific	Cat # A-21202
Rabbit monoclonal IgG isotype control, clone EPR25A	Abcam	Cat # ab172730
Mouse monoclonal IgG1 isotype control, clone G3A1	Cell Signaling Technology	Cat # 5415
HRP-linked anti-rabbit IgG secondary antibody	Cell Signaling Technology	Cat # 7074
HRP-linked anti-mouse IgG secondary antibody	Cell Signaling Technology	Cat # 7076
Cell lines and primary cells		
HEK293 cells	ATCC	CRL-1573
Human pulmonary microvascular endothelial cells (HPMECs)	ScienCell	Cat # 3000
Human pulmonary arterial endothelial cells (HPAECs)	ScienCell	Cat # 3100
Experimental models: organisms/strains		
Mouse: C57BL/6-Tg(Cdh5-cre/ERT2)1Rha	Taconic Biosciences	RRID:IMSR_TAC:13073
Mouse: B6(Cg)-*Mir23a*$^{tm1.1Qjl}$/J	The Jackson Laboratory	RRID:IMSR_JAX:032430
Mouse: B6.129-*Hif1a*^{tm3Rsjo}/J	The Jackson Laboratory	RRID:IMSR_JAX:007561
Mouse: STOCK *Epas1*^{tm1Mcs}/J	The Jackson Laboratory	RRID:IMSR_JAX:008407
Mouse: B6.129S6(C)-*Gt(ROSA)26Sor*$^{tm3(HIF1A*)Kael}$/J	The Jackson Laboratory	RRID:IMSR_JAX:009673
Mouse: STOCK *Gt(ROSA)26Sor*$^{tm4(HIF2A*)Kael}$/J	The Jackson Laboratory	RRID:IMSR_JAX:009674
Mouse: C57BL/6JCya-*Egln2*^{em1flox}/Cya	Cyagen Biosciences	S-CKO-00922
Mouse: B6.129P2(FVB)-*Lyz2*$^{tm1(cre/ERT2)Grtn}$/J	The Jackson Laboratory	RRID:IMSR_JAX:032291
Mouse: B6.129S-*Sftpctm1*$^{(cre/ERT2)Blh}$/J	The Jackson Laboratory	RRID:IMSR_JAX:028054
Mouse: FVB.129S6-*Gt(ROSA)26Sor*$^{tm2(HIF1A/luc)Kael}$/J	The Jackson Laboratory	RRID:IMSR_JAX:006206
Mouse: Rosa26$^{LSL\text{-}Phd1\text{-}3'\ UTR\text{-}WT}$	Cyagen Biosciences	Custom C57BL/6 Cre-inducible *Phd1* 3′ UTR-WT knock-in line; no public catalog number
Mouse: Rosa26$^{LSL\text{-}Phd1\text{-}3'\ UTR\text{-}Mut}$	Cyagen Biosciences	Custom C57BL/6 Cre-inducible miR-23a-3p seed-mutant *Phd1* 3′ UTR knock-in line; no public catalog number

Recombinant DNA and viral vectors		
pcDNA3 *mHIF-2α* MYC P405A/P530V/N851A	Addgene	Plasmid # 44027
pcDNA3 *mHIF-1α* MYC P402A/P577A/N813A	Addgene	Plasmid # 44028
AAV9-GFP-U6-scramble shRNA control (shCon)	Vector BioLabs	Cat # 7045
AAV-h-HIF1A-shRNA (shHIF1A), human	Vector BioLabs	Cat # shAAV-230457; packaged as AAV9
AAV-h-EPAS1/HIF2A-shRNA (shHIF2A), human	Vector BioLabs	Cat # shAAV-207955; packaged as AAV9
Oligonucleotides and RNA reagents		
mirVana miRNA Mimic Negative Control #1	Thermo Fisher Scientific	Cat # 4464060
mirVana miRNA mimic, hsa/mmu/rno-miR-23a-3p	Thermo Fisher Scientific	Assay ID MC10644; Cat # 4464066
TaqMan MicroRNA Assays	Applied Biosystems/Thermo Fisher Scientific	Cat # 4427975
anti-miR-23a-3p LNA inhibitor, mouse	QIAGEN	GeneGlobe ID: YI04103407
hsa-miR-23a-3p LNA inhibitor	QIAGEN	GeneGlobe ID: YI04103406
Negative control LNA miRNA Inhibitor	QIAGEN	GeneGlobe ID: YI00199006
In situ hybridization probes		
miRNAscope LS Probe SR-hsa-miR-23a-3p-S1	Advanced Cell Diagnostics (ACD)/Bio-Techne	Cat # 893318-S1
Chemicals, drugs and commercial reagents		
Lipopolysaccharide from Escherichia coli O111:B4	Sigma-Aldrich	Cat # L4391
Tamoxifen	Cayman Chemical	Cat # 13258
Corn oil	Sigma-Aldrich	Cat # C8267
Roxadustat/FG-4592	MedChemExpress	Cat # HY-13426
Carboxymethylcellulose sodium salt	Sigma-Aldrich	Cat # C5678
Clodronate liposomes with PBS control liposomes	Liposoma BV	Cat # CP-005-005
1,2-dioleoyl-sn-glycero-3-phosphocholine (DOPC)	Avanti Polar Lipids	Cat # 850375
14:0 PEG2000 PE / C14-PEG2000	Avanti Polar Lipids	Cat # 880150
Sevoflurane, USP	Baxter Healthcare	Cat # NDC 10019-653-64
Ethiqa XR (buprenorphine extended-release injectable suspension)	Fidelis Animal Health	Cat # NDC 86084-100-30
Sterile saline	Baxter Healthcare	Cat # 2B1307
DAPI	Thermo Fisher Scientific	Cat # D1306
Antifade mounting medium	Thermo Fisher Scientific	Cat # P36930

Sterile PBS, pH 7.4, without calcium or magnesium	Gibco/Thermo Fisher Scientific	Cat # 10010023
HBSS with calcium and magnesium, no phenol red	Gibco/Thermo Fisher Scientific	Cat # 14025092
Collagenase Type I	Worthington Biochemical Corporation	Cat # LS004196
Bovine serum albumin (BSA)	Sigma-Aldrich	Cat # A9647
Dispase, 5 U/ml	STEMCELL Technologies	Cat # 07913
Low-melting-point agarose	Sigma-Aldrich	Cat # A9414
DNase I	Sigma-Aldrich	Cat # DN25
RBC Lysis Buffer, 10×	BioLegend	Cat # 420301
ACK Lysing Buffer	Gibco/Thermo Fisher Scientific	Cat # A1049201
DMEM, high glucose	Gibco/Thermo Fisher Scientific	Cat # 11965092
Heat-inactivated fetal bovine serum	GenDEPOT	Cat # F0601-050
Heat-inactivated fetal bovine serum for FACS buffer	Gibco/Thermo Fisher Scientific	Cat # 16140071
Penicillin–streptomycin	Gibco/Thermo Fisher Scientific	Cat # 15140122
Recombinant murine M-CSF	Thermo Fisher Scientific	Cat # 315-02
Dimethyloxalylglycine (DMOG)	Sigma-Aldrich	Cat # D3695
7C1 polymer	Clearsynth	Cat # CS-O-49308
tert-Butanol	Sigma-Aldrich	Cat # 471712
Tween-20	Sigma-Aldrich	Cat # P9416
Recombinant human TNF-α	R&D Systems/Bio-Techne	Cat # 210-TA
Lipofectamine RNAiMAX Transfection Reagent	Invitrogen/Thermo Fisher Scientific	Cat # 13778075
Lipofectamine 3000 Transfection Reagent	Invitrogen/Thermo Fisher Scientific	Cat # L3000015
FITC-dextran, 70 kDa	Sigma-Aldrich	Cat # 46945
Rat tail collagen I	Corning	Cat # 354236
EDTA	Invitrogen/Thermo Fisher Scientific	Cat # 15575020
K2-EDTA-coated microcollection tubes	BD Microtainer / Becton Dickinson	Cat # 365974
Fisher Healthcare PROTOCOL Hema 3 Manual Staining System and Stat Pack	Fisher Scientific	Cat # 22-122911
TRIzol Reagent	Invitrogen/Thermo Fisher Scientific	Cat # 15596026
10% neutral-buffered formalin	Sigma-Aldrich	Cat # HT501128
IVISbrite D-Luciferin RediJect Solution, 30 mg/ml	Revvity	Cat # 770504

RIPA Lysis and Extraction Buffer	Thermo Fisher Scientific	Cat # 89900
Protease Inhibitor Cocktail	Thermo Fisher Scientific	Cat # 78425
Phosphatase Inhibitor Cocktail	Thermo Fisher Scientific	Cat # 78420
Pierce BCA Protein Assay Kit	Thermo Fisher Scientific	Cat # 23225
Paraformaldehyde	Millipore Sigma	Cat # P6148
Heparin	StemCell Technologies	Cat # 07980
Trypsin-EDTA	Thermo Fisher Scientific	Cat # 15400054
PVDF membrane	Millipore	Cat # IPVH00010
4-0 nylon suture	Ethicon	Cat # 1662G
21 G needle	BD Biosciences	Cat # 305165
Criterion XT Bis-Tris Protein Gel	Bio-Rad	Cat # 3450124
CD45 MicroBeads, mouse	Miltenyi Biotec	Cat # 130-052-301
CD146 (LSEC) MicroBeads, mouse	Miltenyi Biotec	Cat # 130-092-007
FcR Blocking Reagent, mouse	Miltenyi Biotec	Cat # 130-092-575
LD Columns	Miltenyi Biotec	Cat # 130-042-901
LS Columns	Miltenyi Biotec	Cat # 130-042-401
Pre-Separation Filters, 30 μm	Miltenyi Biotec	Cat # 130-041-407
70-μm cell strainer	Falcon	Cat # 352350
ECL substrate	Thermo Fisher Scientific	Cat # 34580
Kits and commercial assays		
Endothelial Cell Medium kit	ScienCell Research Laboratories	Cat # 1001
MycoAlert Mycoplasma Detection Kit	Lonza	Cat # LT07-318
EasySep Mouse Streptavidin RapidSpheres	STEMCELL Technologies	Cat # 19860
EasySep Magnet	STEMCELL Technologies	Cat # 18000
RNeasy Mini Kit	QIAGEN	Cat # 74106
miRNeasy Mini Kit	QIAGEN	Cat # 217004
High-Capacity cDNA Reverse Transcription Kit	Applied Biosystems/Thermo Fisher Scientific	Cat # 4368814
QuantiTect SYBR Green PCR Kit	QIAGEN	Cat # 204145
TaqMan MicroRNA Reverse Transcription Kit	Applied Biosystems/Thermo Fisher Scientific	Cat # 4366596
TaqMan Universal PCR Master Mix, no AmpErase UNG	Applied Biosystems/Thermo Fisher Scientific	Cat # 4324018
RNAscope Plus smRNA-RNA LS Reagents Kit	Advanced Cell Diagnostics (ACD)/Bio-Techne	Cat # 322786
SimpleChIP Enzymatic Chromatin IP Kit (Agarose Beads)	Cell Signaling Technology	Cat # 9002
Secrete-Pair Dual Luminescence Assay Kit	GeneCopoeia	Cat # LF031
Mouse Albumin ELISA Kit	Bethyl Laboratories	Cat # E99-134

Mouse IL-1β/IL-1F2 Quantikine ELISA Kit	R&D Systems/Bio-Techne	Cat # MLB00C
Mouse IL-6 Quantikine ELISA Kit	R&D Systems/Bio-Techne	Cat # M6000B
Mouse/Rat Angiopoietin-2 Quantikine ELISA Kit	R&D Systems/Bio-Techne	Cat # MANG20
Mouse Syndecan-1/CD138 ELISA Kit	Novus Biologicals/Bio-Techne	Cat # NBP2-76610
Mouse Thrombomodulin/BDCA-3 Quantikine ELISA Kit	R&D Systems/Bio-Techne	Cat # MTHBD0
Transwell inserts, 0.4-μm pore polyester membrane	Corning	Cat # 3470
Software and algorithms		
Fiji/ImageJ	NIH	Fiji version 2.1.0
GraphPad Prism	GraphPad Software	Version 10.0 or later
QIAGEN Ingenuity Pathway Analysis (IPA)	QIAGEN Digital Insights	Accessed 2021
TargetScan	TargetScan	miRNA target-prediction resource
miRanda	miRanda	miRNA target-prediction resource
miRDB	miRDB	miRNA target-prediction resource
Gen5 software	BioTek/Agilent	Used with Cytation 5 reader

90

Supplementary Table 6. qPCR assay and primer information

Species	Target	Assay ID or primer sequence (5′–3′)
Human/mouse	miR-23a-3p	Assay ID: 000399; Mature sequence: AUCACAUUGCCAGGGAUUUCC
Human/mouse	miR-23a-5p	Assay ID: 002439; Mature sequence: GGGGUUCCUGGGGAUGGGAUUU
Human/mouse	miR-27a-3p	Assay ID: 000408; Mature sequence: UUCACAGUGGCUAAGUUCCGC
Human/mouse	miR-27a-5p	Assay ID: 002445; Mature sequence: AGGGCUUAGCUGCUUGUGAGCA
Human/mouse	miR-24-3p	Assay ID: 000402; Mature sequence: UGGCUCAGUUCAGCAGGAACAG
Human/mouse	U6 snRNA	Assay ID: 001973
Human	*ACTB*	F: CACCATTGGCAATGAGCGGTTC R: AGGTCTTTGCGGATGTCCACGT
Mouse	*Actb*	F: CATTGCTGACAGGATGCAGAAGG R: TGCTGGAAGGTGGACAGTGAGG
Human	*HIF1A*	F: TATGAGCCAGAAGAACTTTTAGGC R: CACCTCTTTTGGCAAGCATCCTG
Mouse	*Hif1a*	F: CCTGCACTGAATCAAGAGGTTGC R: CCATCAGAAGGACTTGCTGGCT
Human	*EPAS1/HIF2A*	F: CTGTGTCTGAGAAGAGTAACTTCC R: TTGCCATAGGCTGAGGACTCCT
Mouse	*Epas1/Hif2a*	F: GGACAGCAAGACTTTCCTGAGC R: GGTAGAACTCATAGGCAGAGCG
Human	*EGLN1/PHD2*	F: TGAGCAGCATGGACGACCTGAT R: CGTACATAACCCGTTCCATTGCC
Mouse	*Egln1/Phd2*	F: TGAGCAGCATGGACGACCTGAT R: GACATAGCCTGTTCCGTTGCCT
Human	*EGLN2/PHD1*	F: CTGTCTGGTATTTTGATGCCAAGG R: CGGCTGTGATACAGGTACTTGG
Mouse	*Egln2/Phd1*	F: ATGGCTCACGTGGACGCAGTAA R: CATTGCCTGGATAACACGCCAC
Human	*EGLN3/PHD3*	F: GAACAGGTTATGTTCGCCACGTG R: CCCTCTGGAAATATCCGCAGGA
Mouse	*Egln3/Phd3*	F: CAACTTCCTCCTGTCCCTCATC R: CCTGGATAGCAAGCCACCATTG
Human	pri-hsa-miR-23a~27a~24-2	F: GTGTGGTGGCTCCTGCATAT R: CACCTGGAGGGGAGAAAGAG

Species	Target	Assay ID or primer sequence (5′–3′)
Mouse	pri-mmu-miR-23a~27a~24-2 locus readout	F: CTACACTCCGCTCCCACC R: TTGTGACTGGCATCAAATCC
Human	pre-hsa-miR-23a readout	F: CTGGGGTTCCTGGGGAT R: TGGTAATCCCTGGCAATGTG
Human	pre-hsa-miR-27a readout	F: GCAGGGCTTAGCTGCTTG R: GGCGGAACTTAGCCACTGT
Human	pre-hsa-miR-24-2 readout	F: CTCCCGTGCCTACTGAGCT R: CCCTGTTCCTGCTGAACTGAG
Mouse	pre-mmu-miR-23a readout	F: CTGGGGATGGGATTTGCT R: GCACAGGGTCAGTTGGAAAT
Mouse	pre-mmu-miR-27a readout	F: GCAGGGCTTAGCTGCTTG R: GGCGGAACTTAGCCACTGT
Mouse	pre-mmu-miR-24-2 readout	F: CTCCCGTGCCTACTGAGCT R: CCCTGTTCCTGCTGAACTGAG

92

Supplementary Note 3: Uncropped gel blot images for main Figures

Fig. 2a.

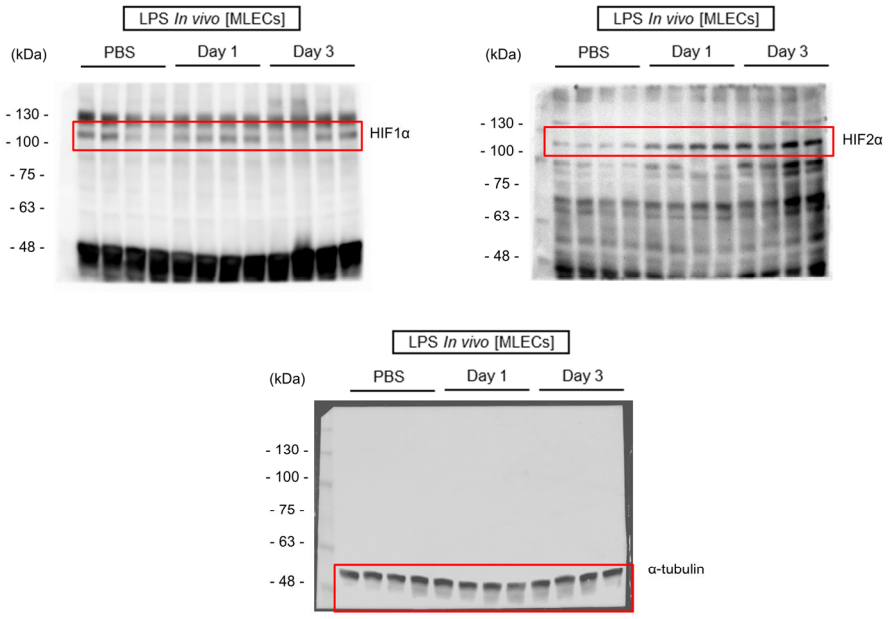

Uncropped western blot (WB) images for Fig. 2a. HIF1α and HIF2α protein levels in MLECs isolated from mice treated with intratracheal PBS or LPS (n = 4 biological replicates). Samples were run on the same gels, with α-tubulin as a loading control.

Fig. 5a.

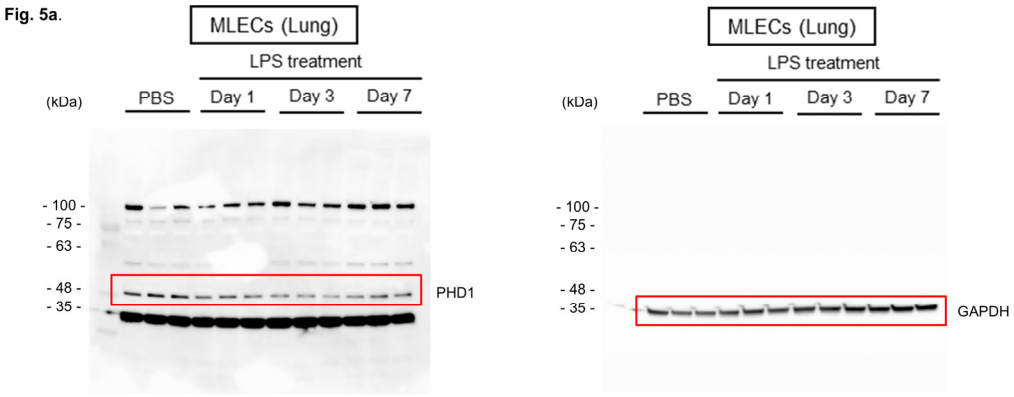

Uncropped WB images for Fig. 5a. PHD1 expression in MLECs isolated from mice treated with intratracheal PBS or LPS (n = 3 biological replicates). Samples were run on the same gels, with GAPDH as a loading control.

Fig. 5f.

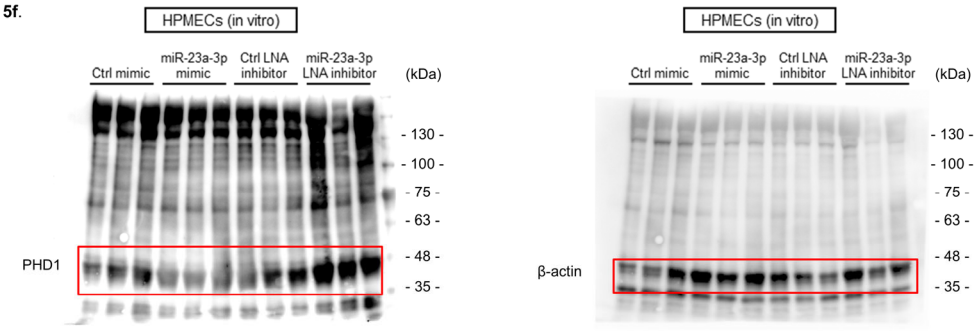

Uncropped WB images for Fig. 5f. PHD1 protein levels in HPMECs transfected with control or miR-23a-3p mimic, or treated with control LNA inhibitor or anti-miR-23a-3p LNA inhibitor (n = 3 biological replicates). Samples were run on the same gels, with β-actin as a loading control.

Fig. 5m.

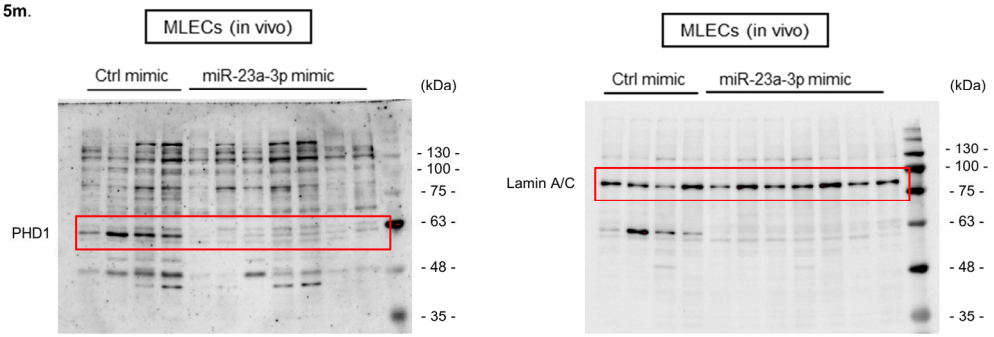

Uncropped WB images for Fig. 5m. MLECs isolated on day 3 after LPS challenge from mice treated with control mimic or miR-23a-3p mimic, and PHD1 protein levels were measured by WB (n = 4 biological replicates for control mimic treated mice and n = 7 biological replicates for miR-23a-3p mimic treated mice). Samples were run on the same gels, with Lamin A/C as a loading control.

Fig. 5o.

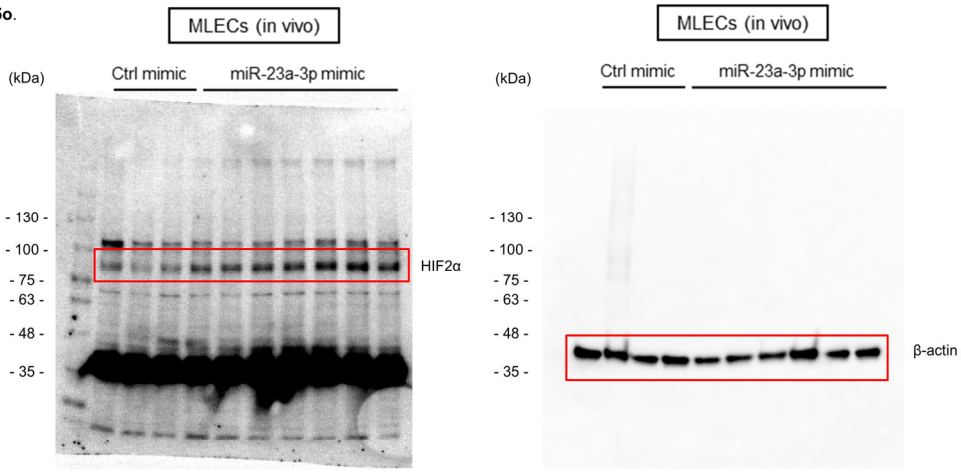

Uncropped WB images for Fig. 5o. MLECs isolated on day 3 after LPS challenge from mice treated with control mimic or miR-23a-3p mimic, and HIF2α protein levels were measured by WB (n = 3 biological replicates for control mimic treated mice and n = 7 biological replicates for miR-23a-3p mimic treated mice). Samples were run on the same gels, with β-actin as a loading control.

Fig. 5r.

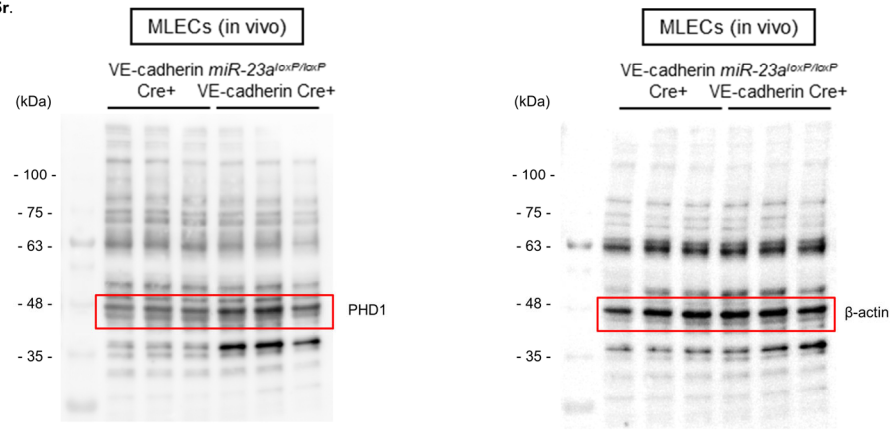

Uncropped WB images for Fig. 5r. MLECs isolated on day 3 after LPS challenge from VE-cadherin Cre+ and *miR-23a*$^{loxP/loxP}$ VE-cadherin Cre+ mice, and PHD1 protein levels were measured by WB (n = 3 biological replicates). Samples were run on the same gels, with β-actin as a loading control.

Fig. 5t.

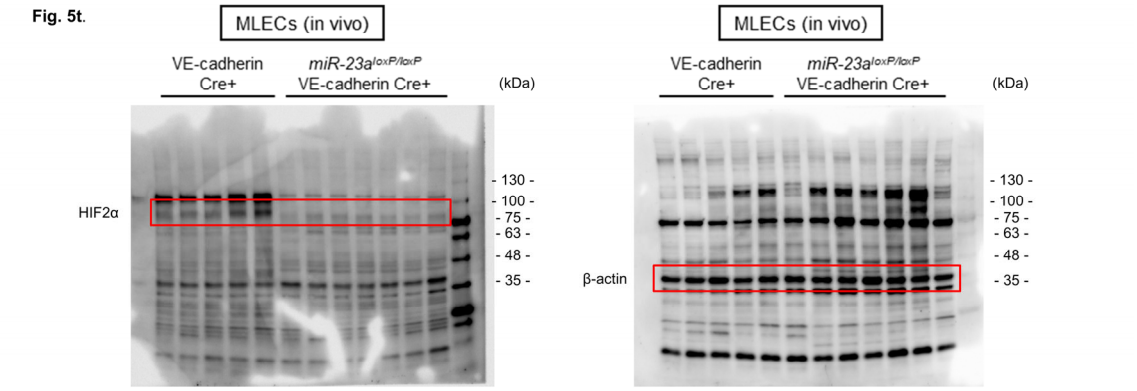

Uncropped WB images for Fig. 5t. MLECs isolated on day 3 after LPS challenge from VE-cadherin Cre+ and *miR-23a*$^{loxP/loxP}$ VE-cadherin Cre+ mice, and HIF2α protein levels were measured by WB (n = 5 biological replicates for VE-cadherin Cre+ mice and n = 7 biological replicates for *miR-23a*$^{loxP/loxP}$ VE-cadherin Cre+ mice). Samples were run on the same gels, with β-actin as a loading control.

Fig. 6j.

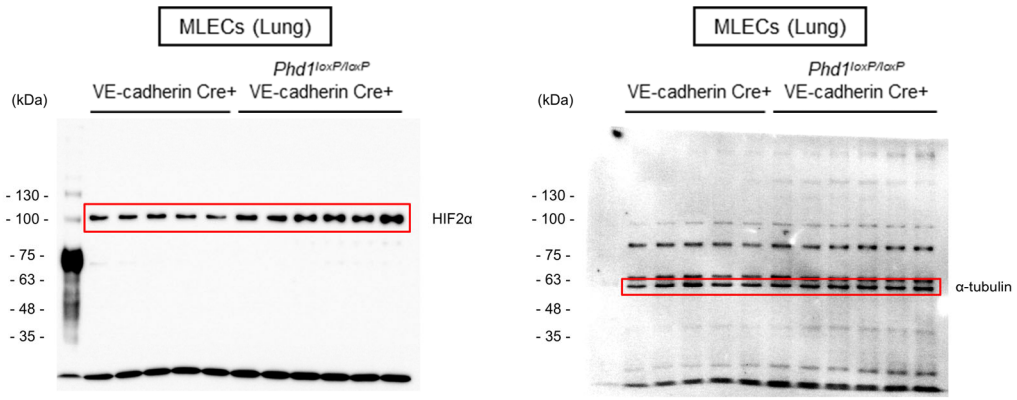

Uncropped WB images for Fig. 6j. VE-cadherin Cre+ and *Phd1*$^{loxP/loxP}$ VE-cadherin Cre+ mice were treated with intratracheal LPS, and HIF2α protein levels were measured by WB in isolated MLECs (n = 5 biological replicates for VE-cadherin Cre+ mice and n = 6 biological replicates for *Phd1*$^{loxP/loxP}$ VE-cadherin Cre+ mice). Samples were run on the same gels, with α-tubulin as a loading control.

Fig. 7b

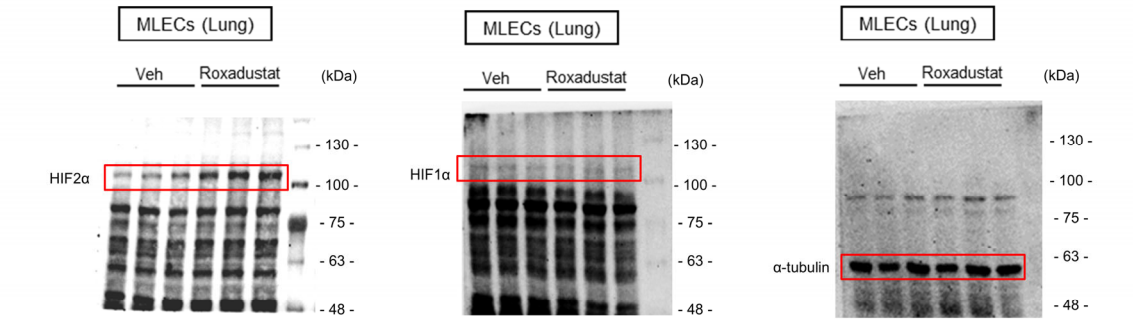

Uncropped WB images for Fig. 7b. C57BL/6J mice were treated with vehicle or roxadustat by oral gavage on consecutive days 1, 2 and 3 after intratracheal LPS challenge, and HIF1α, HIF2α protein levels were measured by WB in isolated MLECs (n = 3 biological replicates). Samples were run on the same gels, with α-tubulin as a loading control.

Fig. 8b.

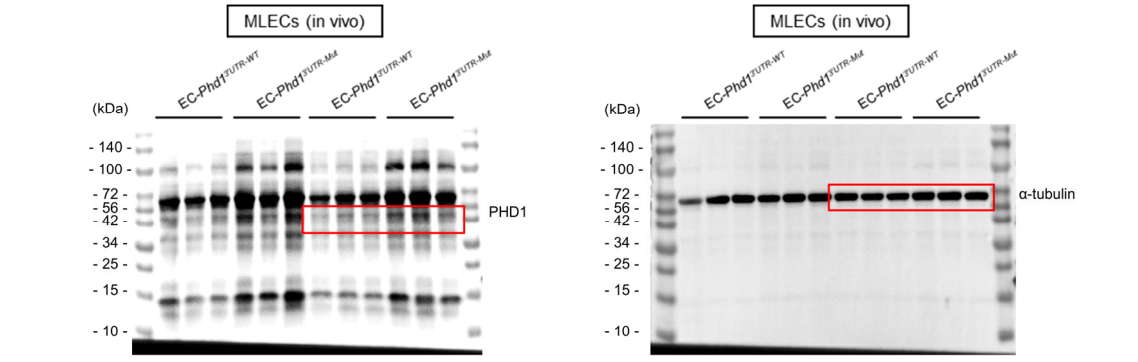

Uncropped WB images for Fig. 8b. EC-*Phd1*$^{3'UTR\text{-}WT}$ and EC-*Phd1*$^{3'UTR\text{-}Mut}$ mice were treated with DOPC-formulated miR-23a-3p mimic on consecutive days 1, 2 and 3 after intratracheal LPS challenge, and PHD1 protein levels were measured by WB in isolated MLECs (n = 6 biological replicates). Samples were run on the same gels, with α-tubulin as a loading control.

Fig. 8f.

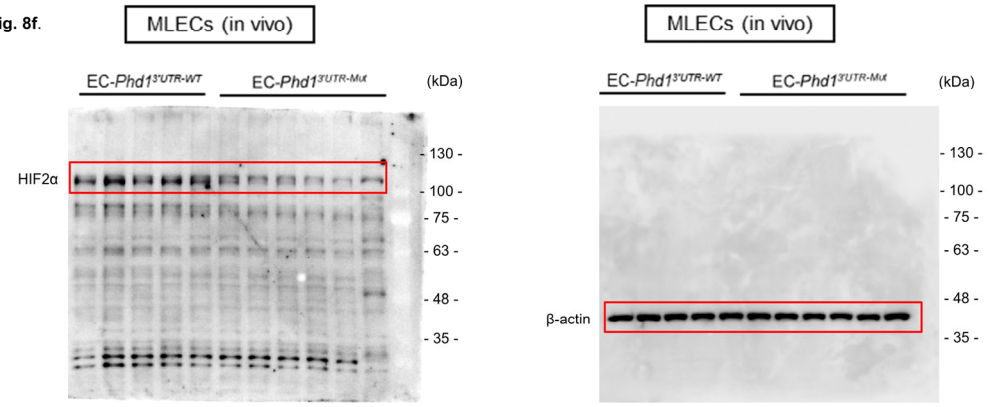

Uncropped WB images for Fig. 8f. EC-*Phd1*$^{3'UTR\text{-}WT}$ and EC-*Phd1*$^{3'UTR\text{-}Mut}$ mice were treated with DOPC-formulated miR-23a-3p mimic on consecutive days 1, 2 and 3 after intratracheal LPS challenge, and HIF2α protein levels were measured by WB in isolated MLECs (n = 5 biological replicates for EC-*Phd1*$^{3'UTR\text{-}WT}$ mice and n = 6 biological replicates for EC-*Phd1*$^{3'UTR\text{-}Mut}$ mice). Samples were run on the same gels, with β-actin as a loading control.

Fig. 9f.

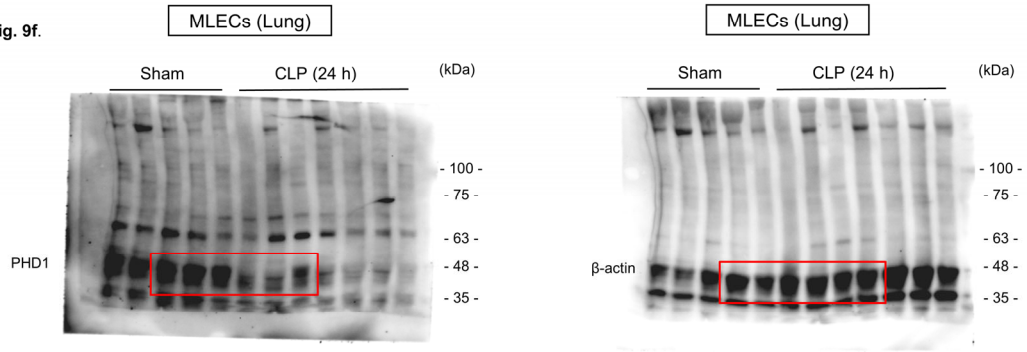

Uncropped WB images for Fig. 9f. PHD1 expression in MLECs after sham surgery or CLP (n = 5 biological replicates for sham-operated mice and n = 7 CLP mice). Samples were run on the same gels, with β-actin as a loading control.

Fig. 9h.

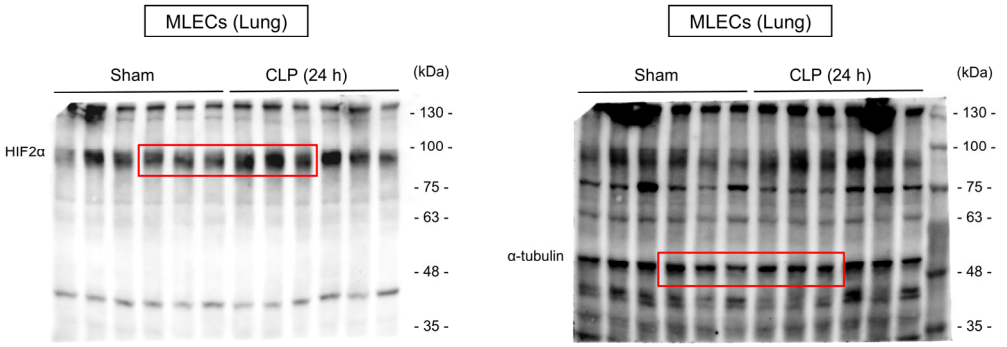

Uncropped WB images for Fig. 9h. HIF2α expression in MLECs after sham surgery or CLP (n = 6 biological replicates). Samples were run on the same gels, with α-tubulin as a loading control.

Fig. 9m.

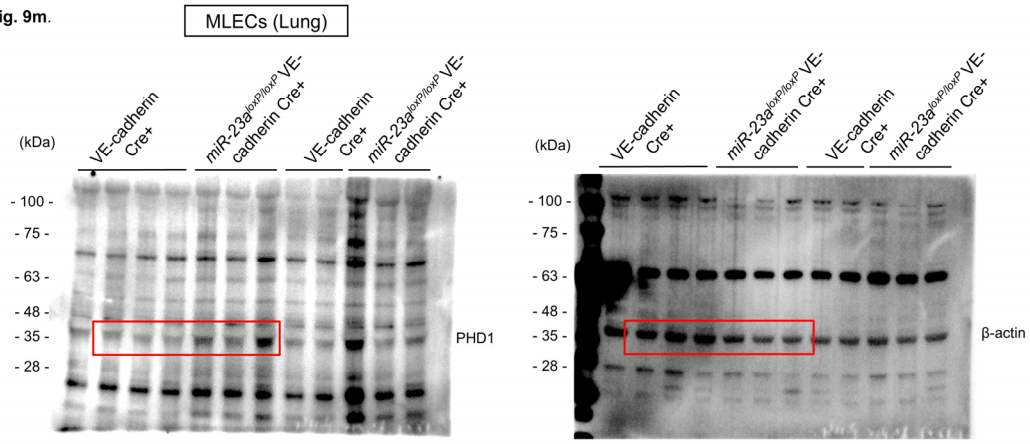

Uncropped WB images for Fig. 9m. VE-cadherin Cre+ and *miR-23a*$^{loxP/loxP}$ VE-cadherin Cre+ mice were subjected to CLP, and PHD1 protein levels were measured by WB in isolated MLECs (n = 6 biological replicates). Samples were run on the same gels, with β-actin as a loading control.

Supplementary Note 4: Uncropped gel blot images for Extended Data Figures.

Extended Data Fig. 2f.

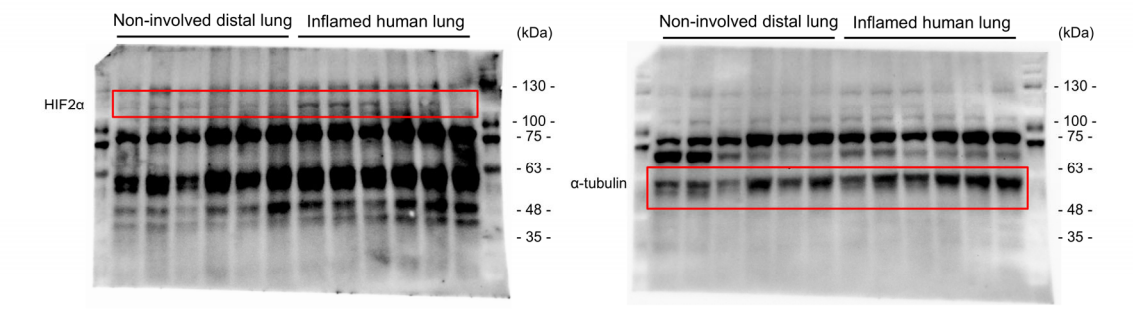

Uncropped WB images for Extended Data Fig. 2f. HIF2α protein levels in human non-involved distal lung tissue and inflamed lung tissue (n = 6 biological replicates). Samples were run on the same gels, with α-tubulin used as the loading control.

Extended Data Fig. 5c.

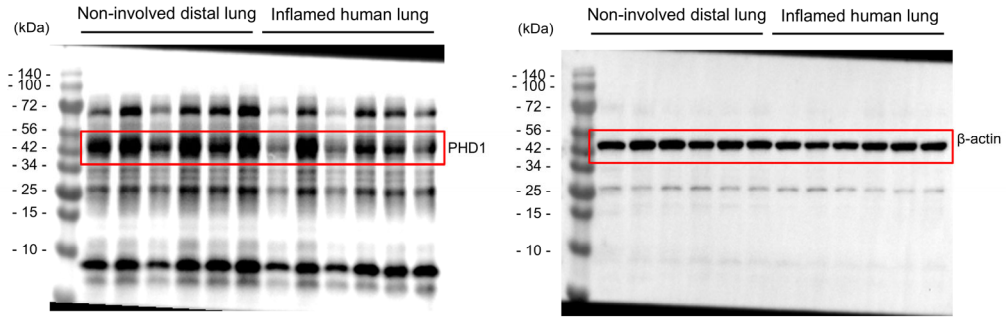

Uncropped WB images for Extended Data Fig. 5c. PHD1 expression in human non-involved distal lung tissue and inflamed lung tissue (n = 6 biological replicates). Samples were run on the same gels, with β-actin as a loading control.

Extended Data Fig. 6c.

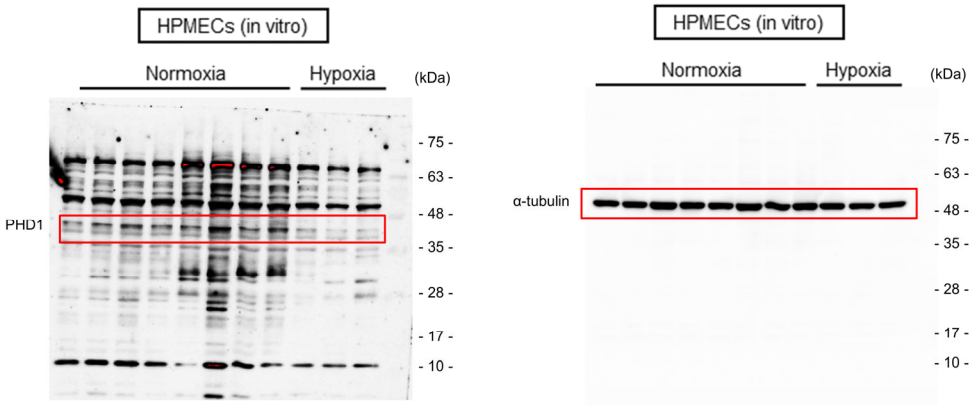

Uncropped WB images for Extended Data Fig. 6c. PHD1 expression in HPMECs exposed to normoxia or hypoxia (n = 8 biological replicates for normoxia-treated cells and n = 3 biological replicates for hypoxia-treated cells). Samples were run on the same gels, with α-tubulin as a loading control.

Extended Data Fig. 8b.

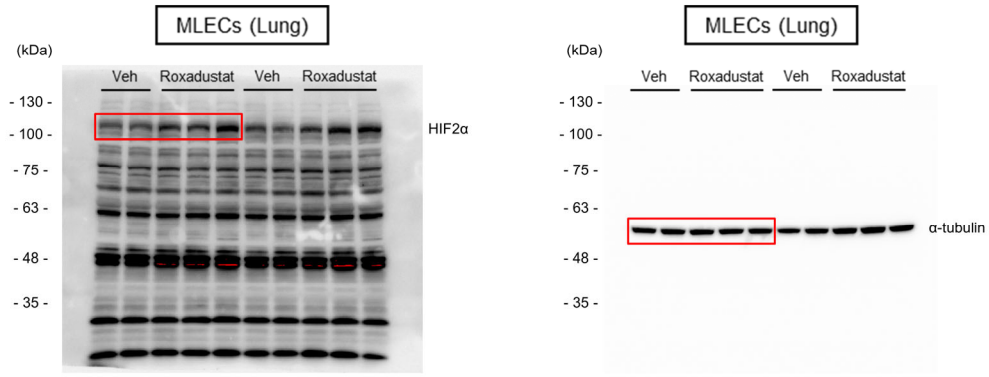

Uncropped WB images for Extended Data Fig. 8b. C57BL/6J mice were treated with vehicle or roxadustat after CLP, and HIF2α protein levels were measured by WB in isolated MLECs (n = 4 biological replicates for vehicle mice and n = 6 biological replicates for roxadustat treated mice). Samples were run on the same gels, with α-tubulin as a loading control.

Supplementary Note 5: Uncropped gel blot images for Supplementary Figures

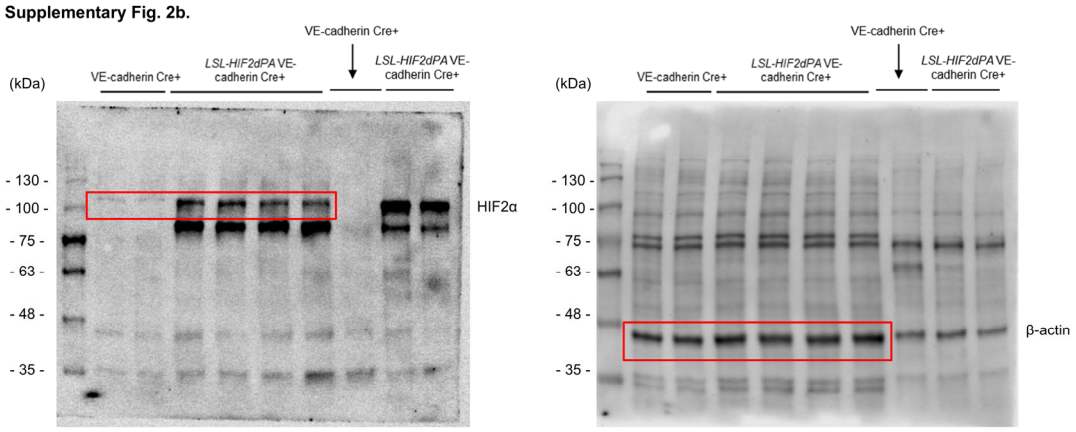

Uncropped WB images for Supplementary Fig. 2b. HIF2α protein levels in isolated MLECs isolated from VE-cadherin Cre+ and *LSL-HIF2dPA* VE-cadherin Cre+ mice (n = 3 biological replicates for VE-cadherin Cre+ mice and n = 6 biological replicates for *LSL-HIF2dPA* VE-cadherin Cre+ mice). Samples were run on the same gels, with β-actin used as the loading control.

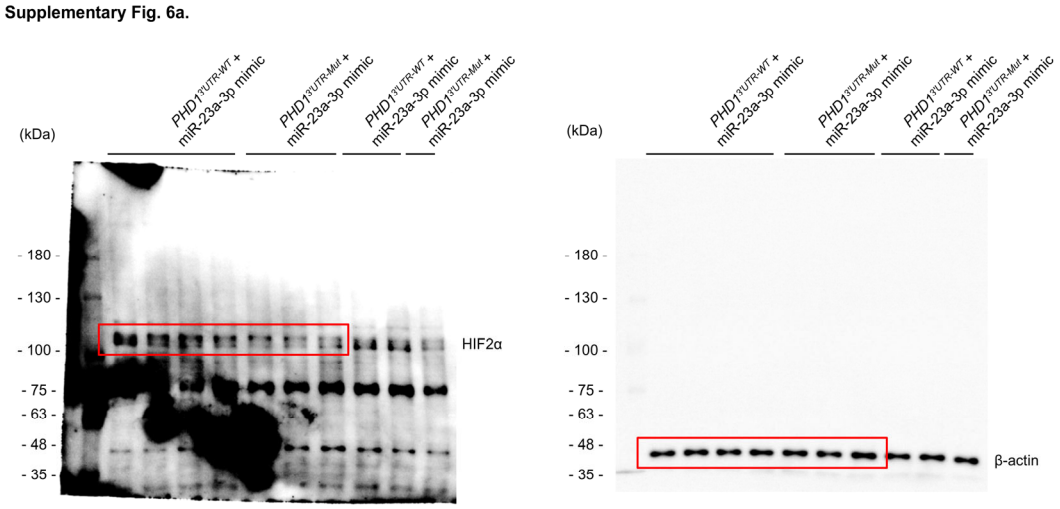

Uncropped WB images for Supplementary Fig. 6a. HIF2α protein levels in HPMECs expressing *PHD1*$^{3'UTR\text{-}WT}$ or *PHD1*$^{3'UTR\text{-}Mut}$ after miR-23a-3p mimic treatment (n = 6 biological replicates for *PHD1*$^{3'UTR\text{-}WT}$ cells and n = 4 biological replicates for *PHD1*$^{3'UTR\text{-}Mut}$ cells). Samples were run on the same gels, with β-actin used as the loading control.